Metallophysics and Advanced Technologies
Металофіз. новітні технол.
Metallofiz. Noveishie Tekhnol.
2024, vol. 46, No. 5, pp. 453–465
https://doi.org/10.15407/mfint.46.05.0453
Reprints available directly from the publisher

PACS numbers: 07.05.Fb, 62.20.Qp, 68.37.Hk, 81.05.ue, 81.40.Pq, 82.80.Ej

Optimization of Multiresponse Process Parameters in Friction Stir Processing of AA6063/*n*-Graphene Composites by Taguchi's Grey Relational Analysis

E. Jenson Joseph, D. Muthukrishnan[*], G. R. Raghav, K. J. Nagarajan[**], and R. Ashok Kumar[***]

SCMS School of Engineering and Technology,
Vidya Nagar, Palissery, Karukutty, Ernakulam,
683582 Kerala, India
[*]*K.L.N. College of Engineering,*
630612 Pottapalayam, Sivagangai District,
Tamil Nadu, India
[**]*Thiagarajar College of Engineering,*
TCE Avaniyapuram Road,
625015 Madurai, Tamil Nadu, India
[***]*SRM Madurai College for Engineering & Technology,*
Nedungulam Main Road,
630611 Madurai, Tamil Nadu, India

The aim of this study is to focus on the multiresponse-process optimization of friction stir processing of AA6063/*n*-graphene-based surface composites to obtain enhanced mechanical properties using Taguchi's technique combined with grey relational analysis (GRA) technique. The parameters of the process selected for this study are tool rotation speed (rpm), tool traverse speed (mm/min), and tilt angle (°). Commonly followed mechanical characterization, namely, hardness and tensile strength are considered as the output performances. The experiments are conducted with a minimal run designed by Taguchi's L_9 orthogonal array factorial design of experiments. GRA is used to optimize the multiresponse-process parameters. In accordance with the analysis, it is found that the specimen synthesized with the tool rotation

Corresponding author: E. Jenson Joseph
E-mail: jenson@scmsgroup.org

Citation: E. Jenson Joseph, D. Muthukrishnan, G. R. Raghav, K. J. Nagarajan, and R. Ashok Kumar, Optimization of Multi Response Process Parameters in Friction Stir Processing of AA6063/*n*-Graphene Composites by Taguchi's Grey Relational Analysis, *Metallofiz. Noveishie Tekhnol.*, **46**, No. 5: 453–465 (2024).
DOI: 10.15407/mfint.46.05.0453

speed of 1200 rpm, traverse speed of 40 mm/min, and 1.5° tilt angle exhibits superior mechanical properties. Analysis of the variance is done to study the dominant factor affecting the strength of the processed composites. SEM analysis with EDX spectrum is done to study the morphological characterization of the prepared composites.

Key words: surface composites, Taguchi's grey relational analysis, friction stir processing, AA6063, *n*-graphene.

Метою даної роботи було проведення оптимізації процесу оброблення тертям з перемішуванням поверхневих композитів на основі AA6063/*n*-графену для одержання поліпшених механічних властивостей за допомогою методики Тагучі в поєднанні з сірою реляційною аналізою (СРА). Параметрами процесу, обраними для цього дослідження, є швидкість обертання інструменту (об./хв.), швидкість переміщення інструменту (мм/хв.) і кут нахилу (°). Загальновідомі механічні характеристики, а саме, твердість і міцність на розрив, вважаються вихідними характеристиками. Експерименти проводилися для мінімальної серії, розробленої за факторіяльною схемою ортогональної матриці Тагучі L_9. СРА використовувалася для оптимізації параметрів процесу з багаторазовим відгуком. Встановлено, що зразок, синтезований зі швидкістю обертання інструменту у 1200 об./хв., швидкістю ходу у 40 мм/хв. і кутом нахилу у 1,5°, демонструє виняткові механічні властивості. Дисперсійну аналізу виконано для вивчення домінувального чинника, що впливає на міцність оброблених композитів. Аналіза скануваною електронною мікроскопією із енергодиперсійним рентґенівським спектром проводиться для вивчення морфологічних характеристик одержаних композитів.

Ключові слова: поверхневі композити, сіра реляційна аналіза за Тагучі, оброблення тертям, AA6063, *n*-графен.

(Received 10 October, 2023; in final version, 10 December, 2023)

1. INTRODUCTION

Aluminium alloys gained much industrial significance due to their unique lightweight properties. Many industries especially automotive and aerospace are concerned the curb weight of the product is a critical factor deciding the fuel efficiency and it could be resolved by employing such lightweight alloys. Composites made of aluminium alloy have significant applications in automobile fields and aerospace due to its lightweight, lesser wear rates, and other enhanced mechanical and thermal properties as compared to the virgin materials [1–8].

Composites based on aluminium matrix can be useful only if it is reinforced with suitable materials that will enhance its properties. Among all the other reinforcements are considered, the carbon-rich reinforcements like carbon nanotubes, graphite, and graphene have unique electrical, mechanical, and thermal properties. Researchers gain the ad-

vantage of the lubricous nature of such carbon materials and taken efforts to synthesize self-lubricating lesser-weight composites that will withstand extreme wear and tear and hence these materials could be employed in automotive and aerospace industries [9–13]. Among these carbon reinforcements, graphene is found to have a cutting-edge advantage over the other materials because to its outstanding optical, mechanical, electrical and thermal properties for varied potential applications. In addition, the honeycomb lattice of single sheet structure in graphene found it to be superior to the other materials [14–16]. Further, the high mechanical strength and high modulus of graphene have gained significant attention in the fabrication of composites.

There are many traditional methods like melting and solidification for fabricating metal matrix composites. However, there are challenges in using the melting and solidification technique for fabricating graphene-reinforced composites. However, graphene has a large surface area, with a lower mass density, which leads to agglomeration during fabrication, and is destroyed by molten metals upon melting. Thus, in order to improve the dispersion of graphene particles, solid-state stirring has been used to fabricate the composite plates.

In the fabrication of aluminium matrix composites, the fabrication methods play a vital role in establishing bonding strength between matrix medium and reinforcement. Hence, selection of fabrication methods is extremely important in determining the mechanical strength of the developed composites. Several fabrication methods are available in the literatures for developing aluminium matrix composites. In recent days, eco-friendly fabrication techniques such as friction stir processing (FSP) have gained much attention among researchers in developing aluminium matrix composites. In FSP, process parameters selection plays a critical role in determining the mechanical strength of the developed composites. The main parameters involved in FSP are tool rotation speed, traverse speed, tool profile and axial load. The impact of these parameters critically affects the properties of metal matrix composites as reported by researchers [12, 17].

The effect of process parameters, on the properties of the developed composites, could be studied by applying a suitable multiresponse optimization tool. The grey relational analysis (GRA) is a suitable multiresponse optimization tool. Aydin *et al.* [18] studied the impact of process parameters on friction welding of AA1050 plates and optimised the process responses using the Taguchi-based GRA. Many researchers used the parametric conventional time-consuming technique where one of the parameters will be varied and all other parameters are kept constant. Hence, to analyse the impact of these parameters by limiting the numbers of experiment runs, a statistical-technique for Taguchi design of experiments could be used. Taguchi's S/N and orthogonal array (OA) are very popular and mostly used for optimization of single response

factor.

Recently, the Taguchi methodology has been integrated with grey relational analysis to solve multiresponse-optimization problems as in the case of friction welding and friction stir processes. Studies conducted by Sureshet *et al.* [19] analysed the effect of tool pin profiles in friction stir welding using Taguchi analysis method, and found that tool rotation speed has more impact on the tensile strength as compared to welding speed and plunging depth.

Pravinet *et al.* [20] investigated the effect of processing parameters on yield strength and tensile strength of friction stir processing of AA606I aluminium alloys and found that titanium carbide shows superior quality of welding at the tool rotation speed of 1500 rpm, tool traverse speed of 25 mm/s and with a square pin profile. Using the Taguchi L_{16} orthogonal design, Koilraj *et al.* [17] conducted FSW studies to optimize process parameters such as tool transverse speed, tool pin shape, rotational speed and D/d ratio.

Vijayan *et al.* [21] investigated the optimization of the FSW process parameters for AA5083 using a L_9 orthogonal array with multiple responses and studied the effect of welding parameters on tensile strength and power with using Taguchi grey relational techniques. Jenson *et al.* [22] used Taguchi combined with grey relational analysis to study the wear characteristics of high-density polyethylene composites with tungsten reinforcement and found that filler content is the dominant factor affecting the wear characteristics of the composites. Hence, Taguchi combined with grey relational analysis will be the suitable tool for the optimization of multiresponse problems.

In this present research, nanographene particles are reinforced into the AA 6063 alloy to form the composite layer. DOE was applied to investigate the effect of process parameters on the mechanical characteristics of the AA6063/n-graphene composites fabricated by friction stir processing. An orthogonal array of L_9 is adopted to find out the impact of process parameters, namely, tool rotational speed, tool traverse speed (mm/min) and tool tilt angle (°) on the hardness and tensile behaviour of AA6063/nanographene composites.

2. MATERIALS AND METHODS

Aluminium AA6063 was selected as the matrix medium, which contains Al–Si–Mg as major composition. The chemical composition of

TABLE 1. Details of the chemical composition of AA6063.

Al	Si	Mg	Mn	Cu	Fe	Zn	Cr	Ni
97.68	0.68	0.88	0.20	0.014	0.30	0.03	0.05	0.007

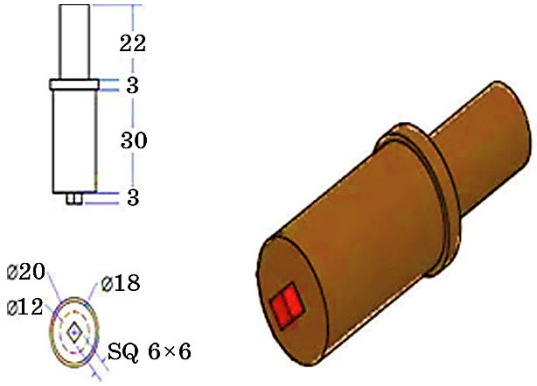

Fig. 1. FSP tool.

AA6063 is derived from XRD analysis shown in the Table 1. The matrix material AA6063 is procured as plates of 6 mm thickness. The specimens were cut by wire cut using electric discharge machining to rectangular sheets of size, 150×50×6 mm. Further, graphene particles of diameter 10 to 15 nm with 10 to 15 layers were purchased from Techinstro, PVT Ltd., Nagpur, were used as reinforcement particles. The tool was fabricated by using a surface grinding and lathe machine. The tool is made of high carbon high chromium (HCHR) of a shoulder diameter 18 mm and attached with a square pin profile of size 6×6 mm and height 3 mm was selected as FSP tool. Square grooves were machined in the centre of the AA6063 specimens (see Fig. 1). The graphene particles are then were filled in the groove. FSP experimentation was conducted using a milling machine with special attachments.

3. RESULTS AND DISCUSSIONS

3.1 Design of Experiments

Friction stir processing of materials were performed with the parameters mentioned in Table 2. Friction stir processing was done with a pinless tool to prevent powder dispersing from the groove during processing. Taguchi L_9 OA designed for this experiment is shown in the Table 3. For each parameter, the plates were rotated 180° to improve powder dispersion and prevent aggregation of powders on the advancing side. The specimens were then machined as per ASTM E8 standards for tensile strength and were tested in universal testing machine and the results are displayed in Table 3. Main effects plot of data mean *vs.* tensile strength and data means *vs.* hardness are plotted using Minitab 16.0 and the results are shown in Figs. 2 and 3.

From Figure 2, it is clear that the tensile strength increases with in-

TABLE 2. FSP parameters.

Parameters	Units	Levels			DOF
		I	II	III	
Tool rotational speed	rpm	900	1200	1500	2
Tool traverse speed	mm/min	20	30	40	2
Tilt angle	Degree	1	1.5	2	2
Total					6

TABLE 3. Experimental results for tensile strength and hardness as per Taguchi L_9 OA.

No.	Process parameters			Processing responses	
	Rotation speed, rpm	Traverse speed, mm/min	Tilt angle, °	Tensile strength, MPa	Hardness
1	900	20	1	179.5	95.7
2	900	30	1.5	183.6	95.2
3	900	40	2	187.3	92.3
4	1200	20	1.5	212.3	123.4
5	1200	30	2	203.45	124.56
6	1200	40	1	215.56	122.45
7	1500	20	2	195.56	117.8
8	1500	30	1	189.67	113.2
9	1500	40	1.5	191.23	110.5

crease in tool rotation speed till 1200 rpm, and then, it decreases and this is because with increase in tool rotation speed the heat generated also increases, which in turn melts a large pool of material and hence a better distribution is possible. Whereas beyond 1200 rpm because of this high heat generation, more metal pool is generated, and hence, the particles are freely movable and so, it will be thrown out due to centrifugal force, and they are clogged in outer area, which causes agglomeration, which causes decreases in the strength of the material.

The tensile strength decreases with the increases in traverse speed and it increases. It is because, initially at less traverse speed, the friction is minimal, and hence, the heat generated will be minimal, which is not sufficient for better distribution of particles. When the traverse speed increases, then, the heat generated also increases which in turn gives a better distribution, which increases the tensile strength. The tensile strength shows only slight variation with the change in tool tilt angle and this is because tool tilt angle do not play significant role in increasing heat generation during processing.

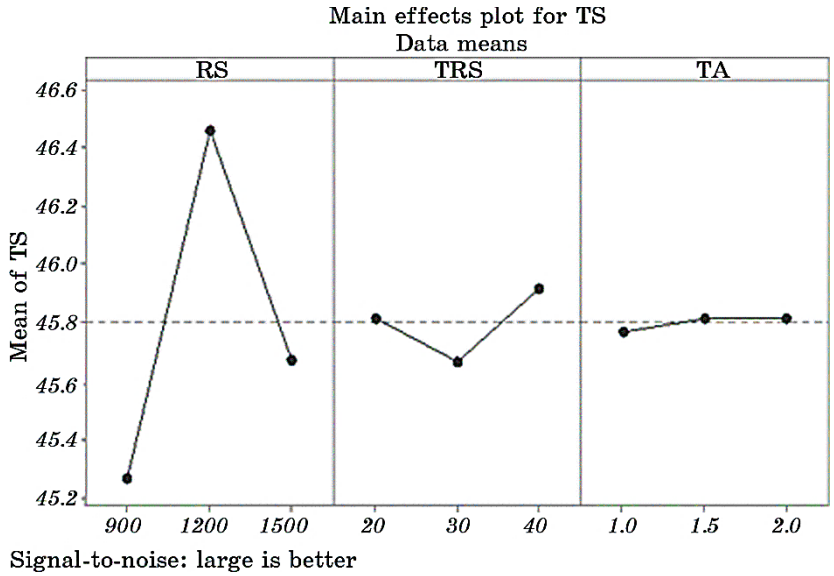

Fig. 2. Main effects plot for tensile strength.

Figure 3 shows that the hardness of the material increases with increase in tool rotation speed till 1200 rpm and beyond that the hardness decreases and it is due to the fact that hardness mainly depends on

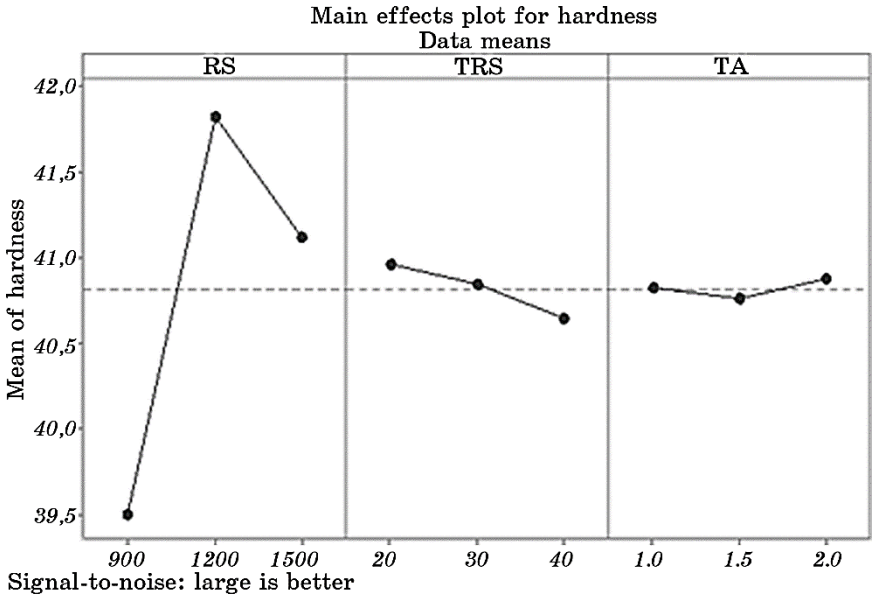

Fig. 3. The main effect plot for hardness.

uniform distribution of reinforcement in matrix medium. With increase in tool rotation speed at 1200 rpm, the distribution is uniform as shown in Fig. 3, and hence, the hardness is high. With increasing the tool rotation speed, the uniform distribution gets affected, and in turn, hardness decreases. Hardness gradually decreases with increase in tool traverse speed, and it is because traverse speed highly affects the uniform distribution of reinforcement and which in turn affects the hardness of the manufactured specimen. Hardness shows only slight variation with tool tilt angle because tool tilt angle do not have much influence on the distribution of reinforcement.

3.2. Grey Relational Analysis

Grey relational analysis is one of the most suitable tools to analyse multiresponse optimization problems. In this study, the optimization of multiple responses is mandatory and hence GRA is adopted. In GRA initially, the data is normalized between 0 and 1 using Eqs. (1) and (2):

$$X_i^* = \frac{\max x_i(k) - x_i(k)}{\max x_i(k) - \min x_i(k)}, \tag{1}$$

$$X_i^* = \frac{x_i(k) - \min x_i(k)}{\max x_i(k) - \min x_i(k)}. \tag{2}$$

Tensile strength and hardness follow the larger the better criteria, hence, Eq. (2) is applied to normalize the data. The normalized values are listed in Table 4. Then, deviation sequence is calculated for the normalized values using Eq. (3):

$$\Delta_{oi}(k) = \left| x_o^*(k) - x_i^*(k) \right|. \tag{3}$$

TABLE 4. Normalised values.

No.	Tensile strength, MPa	Hardness
1	0.000	0.105
2	0.114	0.090
3	0.216	0.000
4	0.910	0.964
5	0.664	1.000
6	1.000	0.935
7	0.445	0.790
8	0.282	0.648
9	0.325	0.564

TABLE 5. Calculated deviation sequence, GRC and GRG.

No.	Deviation sequence		GRC		GRG	RANK
Ideal sequence	Tensile strength	Hardness	Tensile strength	Hardness		
1	1.000	0.895	0.333	0.359	0.346	9
2	0.886	0.910	0.361	0.355	0.358	8
3	0.784	1.000	0.390	0.333	0.361	7
4	0.090	0.036	0.847	0.933	0.890	2
5	0.336	0.000	0.598	1.000	0.799	3
6	0.000	0.065	1.000	0.884	0.919	1
7	0.555	0.210	0.474	0.705	0.589	4
8	0.718	0.352	0.411	0.587	0.499	5
9	0.675	0.436	0.426	0.534	0.480	6

The sequence of deviation calculated using Eq. (3) is displayed in Table 5. The grey relational coefficient (GRC) depicts the relationship between reference and normalised values. GRC is calculated using Eq. (4):

$$\xi_i(k) = \frac{\Delta_{\min} + \xi\Delta_{\max}}{\Delta_{oi}(k) + \xi\Delta_{\max}}. \tag{4}$$

Grey relational grade (GRG) is the mean of GRC and can be calculated using Eq. (5). It provides information on the relationships between the sequences. The range of GRC lies between 0 and 1:

$$\gamma_i = \frac{1}{n}\sum_{k=1}^{n} \xi_i(k). \tag{5}$$

From Table 5, it is evident that experiment number 1 has the highest GRG, and therefore, the optimal sequence to obtain maximum tensile strength and hardness is $A_2B_3C_1$, *i.e.*, with tool rotation speed at 1200 rpm, tool traverse speed at 40 mm/min and tool tilt angle at 1°, it is possible to obtain maximum tensile strength and hardness of the specimen.

Average grey relational grade value for three levels is mentioned in Table 6. From Table 6, it is clear that tool rotation speed of 0.5231 is the most significant factor affecting the strength of the specimen followed by tool traverse speed of 0.0896 and tool tilt angle of 0.0394.

3.3. Analysis of Variance (ANOVA)

For GRG, the sum of squares and all other factors are listed in Table 7. It

TABLE 6. Main effects on mean GRG.

Level	Tool rotation speed (*A*)	Traverse speed (*B*)	Tilt angle (*C*)
1	0.3553	0.6248	0.6083
2	0.8784	0.5353	0.5892
3	0.5327	0.6062	0.5689
Delta	0.5231	0.0896	0.0394
Rank	1	2	3

TABLE 7. ANOVA results on grey relational grade.

Source	Degrees of freedom	Sequence sum of squares	Adjusted sum of squares	Adjusted MS	*F*-value	*P*-value	P.C., %
Tool rotation speed	2	0.424664	0.424664	0.212332	19.28	0.049	91.8
Traverse speed	2	0.013401	0.013401	0.006701	0.61	0.622	2.89
Tilt angle	2	0.002328	0.002328	0.001164	0.11	0.904	0.50
Error	2	0.022022	0.022022	0.011011			4.76
Total	8	0.462415					

is clearly evident from Table 7 that tool rotation speed has a significant contribution of 91.8% affecting the strength of the specimen. Therefore, tool rotation speed is the dominant factor affecting the strength of the specimen. The other factors have only minimal contribution.

3.4. Confirmation Experiment

The results are confirmed by conducting a confirmation test. The optimal value of the multiple factors is predicted using Eq. (6):

$$\gamma = \gamma_{\mathrm{m}} + \sum_{i=1}^{q} (\gamma_i - \gamma_{\mathrm{m}}) . \tag{6}$$

The predicted value and experimental value of GRG is displayed in Table 8. From Table 8, it is found that the predicted value is in line

TABLE 8. Confirmation experiment results.

	Predicted (A2B1C1)	Experiment (A2B1C1)
GRG	0.9341	0.9852

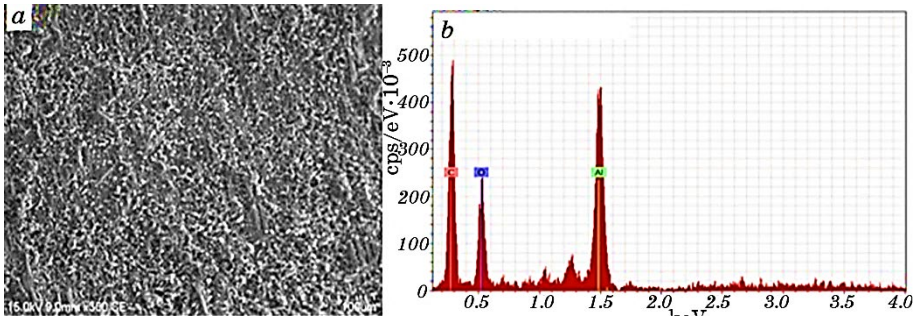

Fig. 4. SEM image (*a*) and EDX spectrum (*b*) of AA6063/*n*-graphene composite, 1200 rpm.

with the experimental value.

3.5. Microstructural Studies

The SEM images of the fabricated AA6063/*n*-graphene surface composites are shown in Fig. 4, *a*. The typical SEM images of AA6063/*n*-graphene surface composites, which are fabricated at the rotational speed of 1200 rpm, is shown in Fig. 4, *a*, which shows the uniform distribution of graphene particles in the matrix.

EDX also confirmed the existence of graphene particles, which are securely fixed within the aluminium matrix to produce a vast interface area. The secure attachment and higher uniformity of graphene particles in the matrix are thought to help the composites' tribological performance due to stress dissipation.

3.6. Microhardness Evaluation

Figure 5 displays the microhardness readings of the specimens processed (FSP) with graphene particles under different rotational speeds (900 rpm, 1200 rpm, and 1500 rpm) at a traverse speed of 20 mm/min. The microhardness of the processed zones is found to be much higher than that of the aluminium matrix AA6063, and the values are rather uniform throughout the processed zones, indicating good graphene particle dispersion in the aluminium matrix. Even though the particles are well dispersed in the matrix after two passes of FSP, the amount of increasing trend is highly minimal, while compared with base metal and processed (FSP) base metal. The value of friction stir processed specimens with particles under three different speeds (900 rpm, 1200 rpm, and 1500 rpm) attained the values of 90 *HV*, 96 *HV*, 125 *HV*, respectively.

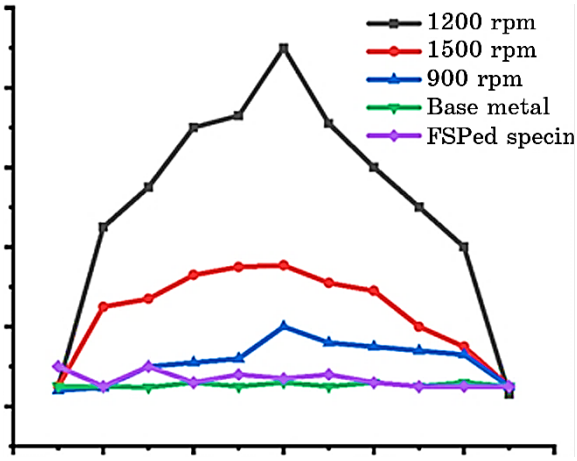

Fig. 5. Microhardness profiles.

The presence of soft graphite phase in all reinforced composites might have resulted in lower hardness values. Further, in this current investigation, processed (FSP) AA6063/nanographene composite under the rotational speed of 1200 rpm showed higher hardness, which is 50% higher than the base metal.

4. CONCLUSION

Friction stir processing of AA6063/*n*-graphene was done successfully. Based on the analysis, following conclusions are drawn. The input parameters were optimized using GRA for getting highest tensile strength and hardness of the specimen. The obtained results are summarized below.

L_9 OA was successfully combined with GRA to optimize the multiple factors.

Observation concludes that the optimal settings to obtain high tensile strength and hardness is A2–B1–C1, *i.e.*, tool rotation speed of 1200 rpm, traverse speed of 20 mm/min and tilt angle of 1° respectively.

From the ANOVA table, it was found that tool rotation is the dominant factor with 95% confidence level affecting the process followed by tool traverse speed and tool tilt angle.

Confirmation experiment shows that the predicted GRG value is in good agreement with the experimental GRG value.

EDX spectrum reveals the presence of AA6063 and *n*-graphene in the composites

SEM analysis shows uniform distribution of *n*-graphene in the matrix of AA6063.

REFERENCES

1. T. Albert, J. Sunil, A. S. Christopher, R. Jegan, P. A. Prabhu, and M. Selvaganesan, *Mater. Today Proc.*, **37**: 1558 (2021).
2. S. Gopinath, M. Prince, and G. R. Raghav, *Mater. Res. Express.*, **7**: 016582 (2020).
3. S. J. Abraham, S. C. R. Madane, I. Dinaharan, and L. J. Baruch, *J. Asian Ceram. Soc.*, **4**, Iss. 4: 381 (2016).
4. N. Karthikeyan, B. R. Krishnan, A. Vembathu Rajesh, and V. Vijayan, *Mater. Today Proc.*, **37**: 2770 (2021).
5. G. Kasirajan, Sathish Rengarajan, R. Ashok Kumar, G. R. Raghav, V. S. Rao, and K. J. Nagarajan, *Met. Res. Technol.*, **117**, No. 4: 405 (2020).
6. F. Khodabakhshi, S. M. Arab, P. Švec, and A. P. Gerlich, *Mater. Charact.*, **132**: 92 (2017).
7. V. Msomi, S. Mabuwa, O. Muribwathoho, and S. S. Motshwanedi, *Mater. Today Proc.*, **46**: 638 (2021).
8. Z. Y. Ma, *Metall. Mater. Trans. A*, **39**: 642 (2008).
9. V. Khanna, V. Kumar, and S. A. Bansal, *Mater. Res. Bull.*, **138**: 111224 (2021).
10. S. M. A. K. Mohammed, D. L. Chen, Z. Y. Liu, D. R. Ni, Q. Z. Wang, B. L. Xiao, and Z. Y. Ma, *Mater. Sci. Eng. A*, **817**: 141370 (2021).
11. K. G. Thirugnanasambantham, T. Sankaramoorthy, M. Vaysakh, S. Y. Nadish, and D. Nilesh Sabarinath, *Mater. Today Proc.*, **45**: 2606 (2021).
12. M. Wang, Y. Li, B. Chen, D. Shi, J. Umeda, K. Kondoh, and J. Shen, *Mater. Sci. Eng. A*, **808**: 140893 (2021).
13. V. S. Aigbodion, *Chem. Data Collect.*, **33**: 100707 (2021).
14. A. Radha and K. R. Vijayakumar, *Mater. Today Proc.*, **3**: 2247 (2016).
15. S. Stankovich, D. A. Dikin, G. H. B. Dommett, K. M. Kohlhaas, E. J. Zimney, E. A. Stach, R. D. Piner, S. T. Nguyen, and R. S. Ruoff, *Nature*, **442**: 282 (2006).
16. R. Sadri, M. Hosseini, S. N. Kazi, S. Bagheri, S. M. Ahmed, G. Ahmadi, N. Zubir, M. Sayuti, and M. Dahari, *Energy Convers. Manag.*, **150**: 26 (2017).
17. M. Koilraj, V. Sundareswaran, S. Vijayan, and S. R. Koteswara Rao, *Mater. Des.*, **42**: 1 (2012).
18. H. Aydin, A. Bayram, U. Esme, Y. Kazancoglu, and O. Guven, *Mater. Tehnol.*, **44**, No. 4: 205 (2010).
19. S. Ko, H. Park, Y.-H. Lee, S. Shin, I. Jo, J. Kim, S.-B. Lee, Y. Kim, S.-K. Lee, and S. Cho, *Mater.*, **13**, Iss. 7: 1588 (2020).
20. T. Pravin, C. Somu, R. Rajavel, M. Subramanian, and P. Prince Reynold, *Mater. Today Proc.*, **33**: 5156 (2020).
21. S. Vijayan, R. Raju, and S. R. K. Rao, *Mater. Manuf. Process.*, **25**, Iss. 11: 1206 (2010).
22. E. J. Joseph and K. Panneerselvam, *Mater. Today Proc.*, **46**: 9150 (2021).